2.B Hydrodynamic-Efficiency Measurements on Planar Targets

The efficiency with which the laser energy absorbed by the plasma is transferred to the compressed core is one of the most important parameters in laser-driven fusion. Since this quantity is very difficult to deduce experimentally in spherical geometry, we have conducted a series of experiments using planar targets to assess our ability to make accurate predictions of this efficiency. We describe here a set of experiments using thin, planar targets illuminated by 351-nm and 1054-nm laser light, in which we have measured the kinetic energy of the accelerated target mass on the rear side of the target (opposite to the laser).

When using planar targets, one prefers to use sufficiently large spot sizes so that the acceleration is essentially one-dimensional. This condition would require the use of spot sizes greater than 200 μm in radius, and irradiation intensities below 10^{13} W/cm^2, since we unfortunately have only 50-60 J available in one UV beam. These intensities are too low for our future needs, so we chose to use smaller spot sizes, of radius 50-200 μm, and set out to account for the non-planar nature by comparing the experimental results with two-dimensional hydrodynamic computations carried out with the Eulerian code *SAGE*.[1] As will be seen, the agreement between the experimental observations and the predictions of the computer code permits us to interpret these experiments with a certain degree of confidence.

Planar CH foils were irradiated with 1-ns pulses of 351-nm light at intensities typically around 10^{14} W/cm^2, but in some cases as high as 7×10^{14} W/cm^2. The kinetic energy of the unablated target mass was measured on the rear side of the target using two types of plasma calorimeters. One is a relatively small, compensating calorimeter. Because of their small size and their ability to discriminate between plasma and light energy, these devices were used near the target normal at angles out to 32°. Above 32°, the small calorimeters were not sensitive enough to record the low-amplitude signals. Large-aperture calorimeters were used to cover the angular region above 32°. These measurements allow one to measure the integrated energy above 32° but give very little angular resolution. Thus, we may compare the predicted and observed angular distributions up to 32° and the total energy integrated over all angles.

Very strong angular effects associated with small spot sizes are evident in the calculated angular distributions of Fig. 5. In these calculations, inverse-bremsstrahlung absorption was assumed to be the only absorption mechanism, and a thermal-conduction flux limiter of f = 0.04 was used. One notes that for spots of radius 200 μm or greater, almost all the energy is in the forward direction, i.e., normal to the surface. Thus, a one-dimensional planar approximation would be reasonable for such spots. For 120-μm-radius spots, the contributions at angles greater than 10° are already significant, and for radii less than 80 μm the expansion is strongly divergent rather than planar.

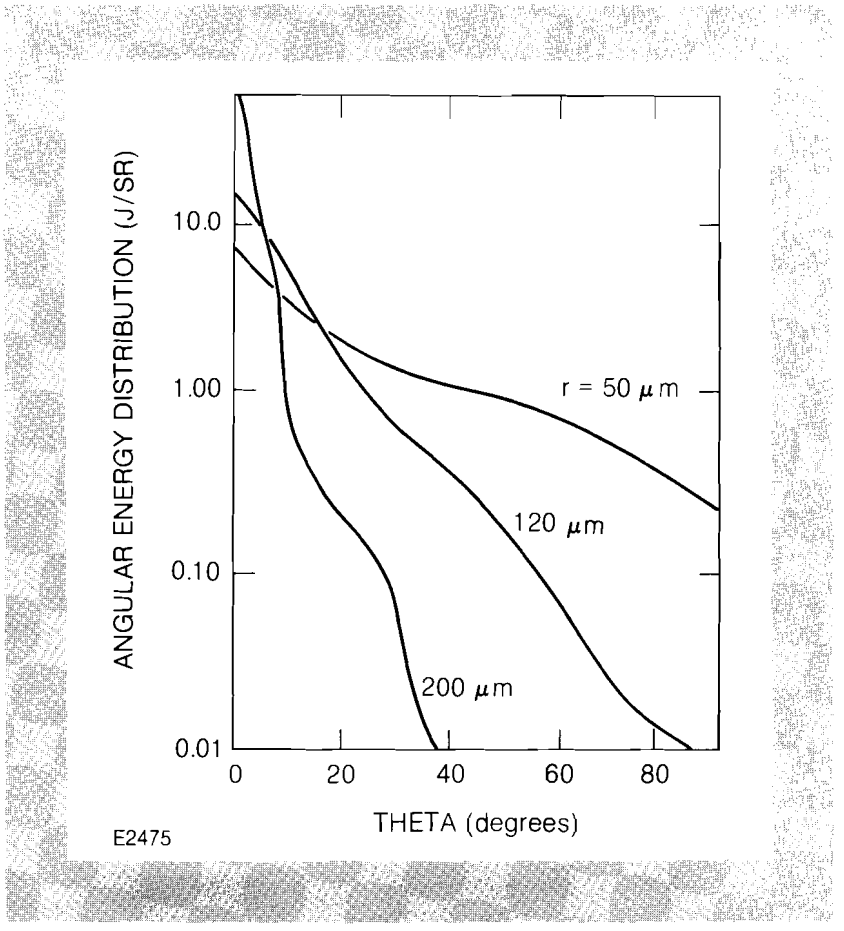

Fig. 5
Predictions of the code SAGE *for the angular energy distribution of the rear plasma blow-off from CH targets irradiated with various spot sizes. Simulations are for 351-nm, 40-J, 1-ns pulses on 10-μm CH targets. The blow-off changes from highly planar to strongly divergent as the spot size decreases.*

Figures 6a and 6b show the satisfactory agreement between the observed and predicted angular distributions for 50-μm- and 100-μm-radius spots.

The experimental data for the 100-μm-radius case are adequately modeled by using the 120-μm-radius code calculation. We have determined that the intensity distribution changes from nearly Gaussian at best focus to a ring-like structure at larger spot radii. The 100-μm-radius spot is located just below the transition region. As shown, the code can satisfactorily model the shots with small spots using a uniform intensity distribution. However, in modeling shots with a radius greater than 200 μm the code predicts planar-like blow-off, whereas in the experiment the blow-off still retains its divergent nature. We have found that the intensity distribution can affect the shape of the rear blow-off. Small-scale beam intensity variations can accelerate material a distance comparable to the local intensity scale length during the laser pulse. The result is a locally divergent expansion which will affect the overall shape of the blow-off. Code calculations for a ring intensity distribution demonstrate this result. Figure 7a shows density contour plots and ray trajectories for a uniform intensity distribution at two different times during the irradiation. Figure 7b shows similar data using a ring intensity distribution. The annular ring leads to a more divergent expansion, contributing to significant amounts of energy at large angles with respect to the target normal.

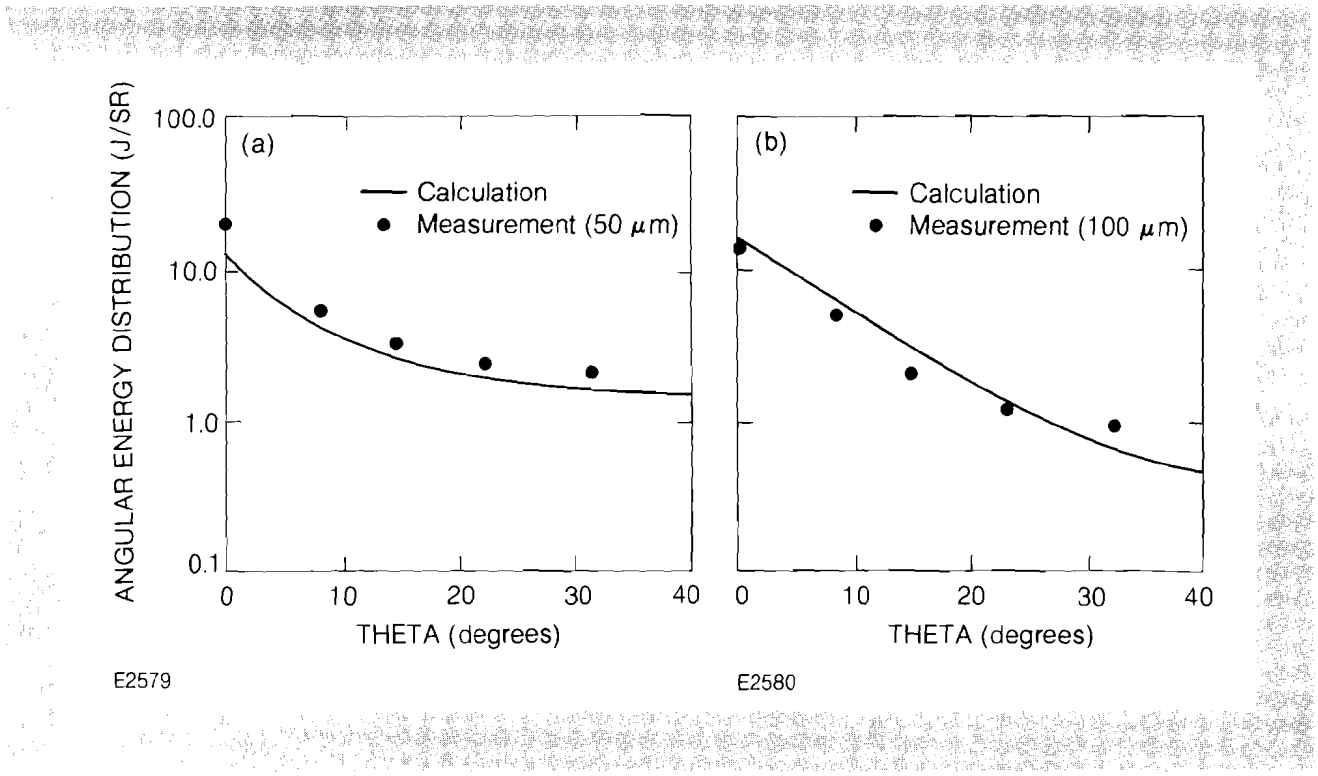

Fig. 6
Comparison between code predictions and experiments for the rear plasma energy distribution for (a) small (50-μm radius) spots and (b) 100-μm spots. The 10-μm-thick CH targets are irradiated with 1-ns pulses of 351-nm light. [In case (b) a spot radius of 120 μm was assumed in the calculation.]

The ability to model large-spot experiments correctly depends on the ability to characterize the intensity distribution of the focal spot.

Figure 8 shows the measured hydrodynamic efficiency (plasma kinetic energy divided by absorbed energy) versus absorbed intensity for constant target thickness and for 351-nm and 1054-nm irradiation. The absorption fractions used in order to plot the experimental data were taken from LLE measurements on thick plastic targets for 351-nm radiation,[2] and from the *SAGE* calculations for 1054-nm radiation.

A close correlation is seen in Fig. 8 between the observed and calculated efficiencies, at both wavelengths and across a broad intensity range. The agreement at the high-intensity end of the 351-nm curve should, however, be treated with caution, since the code predicts significant transmission of laser energy (>8% at incident intensities above 3×10^{14} W/cm^2) which has not been observed in these experiments.

Caution should also be exercised in comparing the hydrodynamic efficiencies measured at the two different wavelengths: on account of the much-reduced mass-ablation rate at 1054 nm, the 10-μ target thickness was above the optimum for 1054-nm radiation. It is still worth noting that, for 351-nm radiation and at incident intensities a few times 10^{14} W/cm^2 (where the absorption efficiency is $\approx$ 80%[2]), ~ 20% of the incident energy may be converted into kinetic energy of the accelerated target.

Finally in Fig. 9 we show the variation of the hydrodynamic efficiency with target thickness keeping the intensity constant (at

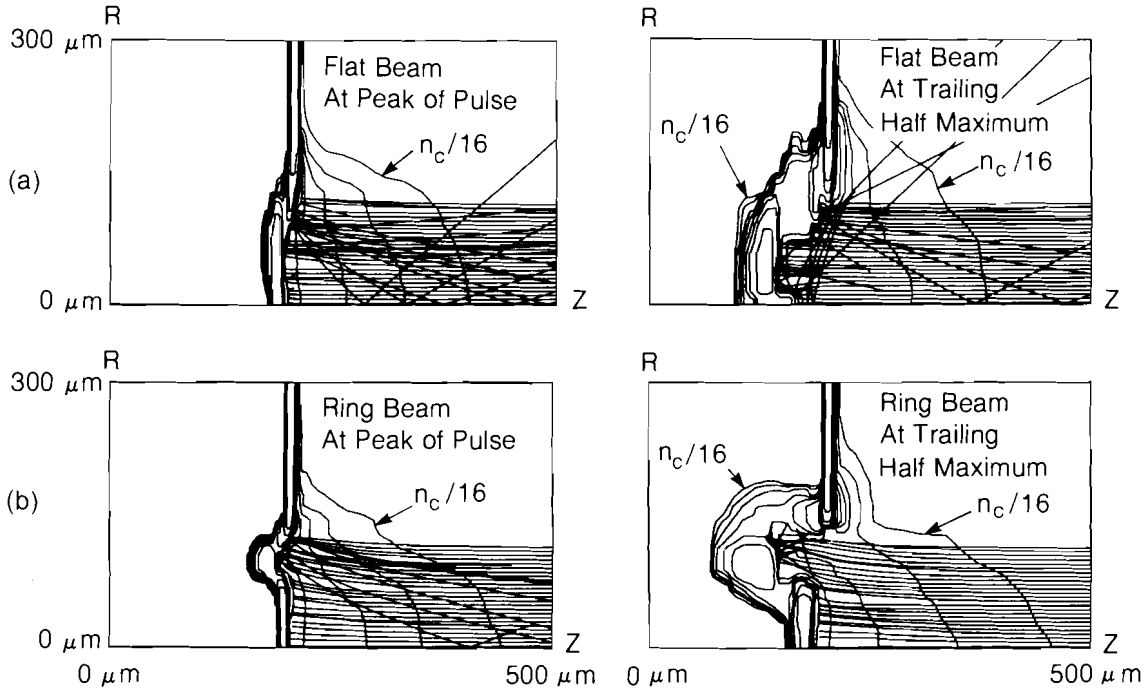

RUNS 1089, 1091
TC1513

Fig. 7
Electron density contours and ray trajectories calculated by SAGE *for 10-μm CH targets irradiated with 1-ns pulses of 351-nm light. The density changes by a factor of 2 between contours. The effect of the focal-spot intensity distribution on the rear blow-off is shown by comparing (a) a uniform intensity distribution at 7.2×10^{13} W/cm² and (b) a ring distribution with a 5:1 (1×10^{14}: 2×10^{13} W/cm²) intensity ratio. Both simulations are for a 10-μm-thick CH target; the contours shown are at the peak and trailing half-maximum of a 1-ns pulse for both cases.*

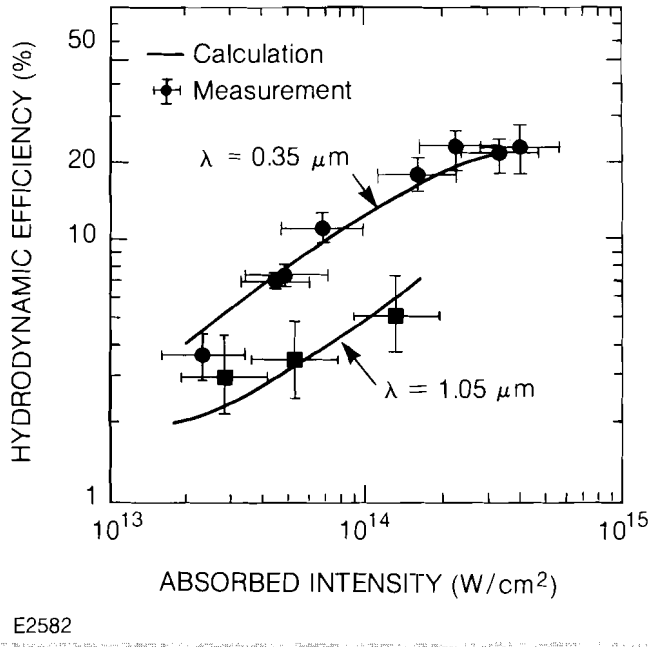

E2582

Fig. 8
Comparison of measured and predicted hydrodynamic efficiency for 10-μm CH targets for various absorbed intensities. The hydrodynamic efficiency is defined relative to the absorbed energy.